

Experimental investigation on durability performance of rubberized concrete

Erhan Güneyisi^{*1}, Mehmet Gesoğlu¹, Kasım Mermerdaş² and Süleyman İpek¹

¹Department of Civil Engineering, Gaziantep University, Gaziantep, Turkey

²Department of Civil Engineering, Hasan Kalyoncu University, Gaziantep, Turkey

(Received February 24, 2014, Revised July 25, 2014, Accepted April 3, 2014)

Abstract. The study presented herein aims to investigate the durability related properties of rubberized concrete. Two types of waste scrap tire rubber were used as fine and coarse aggregate, respectively. The rubber was replaced with aggregate by three crumb rubber and tire chips levels of 5, 15, and 25% for the rubberized concrete productions. In order to improve the transport properties and corrosion resistance of rubberized concretes, SF was replaced with cement at 10% replacement level by weight of total binder content. The transport properties of the rubberized concretes were investigated through water absorption, gas permeability, and water permeability tests. The corrosion behavior of reinforcing bars embedded in plain and silica fume based rubberized concretes was investigated by linear polarization resistance (LPR) test. The results indicated that the utilization of SF in the rubberized concrete production enhanced the corrosion behavior and decreased corrosion current density values. Moreover, the reduction in the water and gas permeability coefficients was observed by the incorporation of SF in plain and especially rubberized concretes.

Keywords: concrete; corrosion resistance; durability; permeability; tire rubber

1. Introduction

Disposal of waste materials is one of the most serious environmental problems all around the world. Waste tire is one of these disposal waste materials. Generally, burning the waste tires has become the cheapest and easiest way to decompose them. The air pollution, however, caused by the release of large amounts of green house gases due to combustion, makes this method so unacceptable that it has also been prohibited by law in many countries (Siddique and Nail 2004, Sukontasukkul and Chaikaew 2006). Utilization of the waste rubber as raw material for rubber products is suggested by some researchers (Eldin and Senouci 1993a). The waste rubbers obtained from the cryogenic milling of tires are also used in the hot mix asphalt pavements as a fine aggregate addition (dry process) and binder modifier (wet process) (Siddique and Nail 2004). Moreover, utilization of waste materials in cement-based composite materials as an additive has been proposed (Rebeiz *et al.* 1992, Rebeiz *et al.* 1993, Rebeiz *et al.* 1994, Wang *et al.* 1994, Wu *et al.* 1996, Segre and Joeques 2000, Soroushian *et al.* 2003, Wang *et al.* 2012, Al-tayeb *et al.* 2013,

*Corresponding author, E-mail: guneyisi@gantep.edu.tr

Issa and Salem 2013, Yung *et al.* 2013). In recent years, some researchers have attempted to use the rubber aggregate in concrete by replacing with some part of natural aggregates (Gesoğlu and Güneyisi 2007, Issa and Salem 2013, Yung *et al.* 2013). In the literature, use of crumb rubber and tire chips as rubber aggregates has found a lot of attention. In many studies, the natural aggregate was replaced with rubber aggregate to investigate effect of rubber on the mechanical performance (Eldin and Senouci 1993a, Eldin and Senouci 1993b, Lee *et al.* 1993, Eldin and Senouci 1994, Topçu 1995, Savaş *et al.* 1996, Toutanji 1996, Topçu 1997, Topçu and Avcular 1997, Li *et al.* 1998, Raghavan *et al.* 1998, Khatip and Bayomy 1999, Ali *et al.* 2000, Rostami *et al.* 2000, Güneyisi *et al.* 2004, Gesoğlu and Güneyisi 2007, Al-tayeb *et al.* 2013, Issa and Salem 2013, Wang *et al.* 2013, Yung *et al.* 2013). The results in these studies indicated that the replacement of the natural aggregate with rubber aggregate decreased the compressive strength. Siddique and Naik (2004) discussed that the size, proportions, and generally surface texture of rubber particles, and type of cement used in rubberized concrete greatly affected the compressive strength of concrete mixtures. The studies on size effect of rubber particles revealed that the compressive strength of concrete produced with only coarse rubber particles was decreased more than produced with fine particles (Eldin and Senouci 1993a, Topçu 1995, Rostami *et al.* 2000).

Several studies showed that the reduction in the strength of concrete is because of adhesion deficiency between the rubber particles and cement paste (Eldin and Senouci 1993a, Topçu 1995, Gesoğlu and Güneyisi 2007, Gesoğlu and Güneyisi 2011, Rahman *et al.* 2012). For that reason, surface treatment was applied on the rubber particles through immersion in NaOH before using in concrete production in an attempt to enhance the adhesion between the rubber and matrix (Eldin and Senouci 1993a, Raghavan *et al.* 1998, Li *et al.* 1998, Segre and Joeke 2000). Generally, this method was used to modify the surface of the rubber particles through immersion in NaOH aqueous solution for increasing its adhesion to the surrounding cement paste. Furthermore, it was reported that by the utilization of ultrafine mineral admixtures such as silica fume, fly ash and rice husk ash, the homogeneity of concrete was increased and the number of large pores in matrix is decreased (Mehta and Gjorv 1982, Feldman and Huang 1985, Mindess 1994, Inthata and Cheerarot 2014, Parande 2013). In the work of Güneyisi *et al.* (2004), silica fume was incorporated to provide a denser interface between the cement paste and rubber aggregate. This study showed that the mechanical properties of concrete containing rubber aggregate were enhanced and the rate of strength loss was diminished by silica fume addition. Although there have been many studies related with the use of waste tire rubber in concrete, the knowledge regarding durability properties of rubberized concrete is still insufficient (Savaş *et al.* 1996, Siddique and Nail 2004, Gesoğlu and Güneyisi 2007, Gesoğlu and Güneyisi 2011).

In this study, the effect of using rubber aggregate on permeability and corrosion behavior of concretes was investigated. For that reason, two types of waste scrap tire rubber, crumb rubber and tire chips, were utilized as an aggregate in concrete with three replacement level of 5, 15, and 25%. Two concrete series with and without silica fume were produced with constant water-to-binder ratio of 0.60 and cement content of 300 kg/m³. Silica fume was replaced with cement at replacement level of 10% by weight. The durability performance of the concrete was determined in terms of transport property and corrosion resistance of steel in concrete. The transport properties of concrete were evaluated using water and gas permeability tests. To evaluate the corrosion rate of concretes, the concrete specimens were exposed to 3% NaCl. The effect of using rubber aggregate and silica fume on corrosion behavior of reinforcing bars embedded in concretes was performed through linear polarization resistance (LPR) test. The results of the tests were discussed comparatively.

2. Experimental

2.1 Materials

The materials used in this investigation were Portland cement, silica fume, fine aggregate, coarse aggregate, waste scrap tire rubber, and superplasticizer. Portland cement (CEM I 42.5R) conforming to the Turkish standard TS EN 197-1 (which mainly based on the European EN 197-1) and commercial grade silica fume (SF) were utilized as a supplementary cementing material. The chemical compositions and physical properties of Portland cement and silica fume are given in Table 1.

The fine aggregate was a mixture of river sand and crushed sand while coarse aggregate was river gravel. The properties of natural aggregates are given in Table 2. Two types of scrap tire rubber obtained from used truck tires castaway after second recapping. Crumb rubber having a specific gravity of 0.83 is a fine material with gradation close to that of the sand and tire chips having a specific gravity of 1.02 are produced by mechanical shredding and include coarser particle sizes. The gradation of crumb rubber was determined based on the ASTM C136 method. Nevertheless, it was not possible to determine the gradation curve for the tire chips, as for normal aggregates since they are elongated particles between 10 and 40 mm. A commercially available sulphonated naphthalene formaldehyde based superplasticizer was used to achieve a consistent workability. Its specific gravity is about 1.18.

2.2 Mix proportions

Two control mixtures were designed at water-to-binder ratio (w/b) of 0.60 with the total binder content of 300 kg/m³. 10% silica fume was used in the mixtures as partial replacement of cement in order to examine the effect of silica fume on durability properties of rubberized concrete. To develop the rubberized concrete mixtures, all mix design parameters were kept constant except for the aggregate content. That is, the cementitious material content, w/b ratio, and aggregate volume

Table 1 Chemical compositions and physical properties of portland cement and silica fume

Material	Portland Cement	Silica Fume
SiO ₂ (%)	19.73	90.36
Al ₂ O ₃ (%)	5.06	0.71
Fe ₂ O ₃ (%)	3.99	1.31
CaO (%)	62.86	0.45
MgO (%)	1.61	-
SO ₃ (%)	2.62	0.41
Na ₂ O (%)	0.18	0.45
K ₂ O (%)	0.80	1.52
Cl (%)	0.01	-
Loss on ignition (%)	1.90	3.11
Specific gravity	3.14	2.20
Fineness (m ² /kg)	327	21080

Table 2 Sieve analysis and physical properties of natural aggregates

Sieve size (mm)	Fine aggregate		Coarse aggregate	
	River sand	Crushed sand	No I (4-16 mm)	No II (16-22 mm)
31.5	100	100	100	100
16.0	100	100	100	27.7
8.0	99.7	100	31.5	0.6
4.0	94.5	99.2	0.4	0
2.0	58.7	62.9	0	0
1.0	38.2	43.7	0	0
0.50	24.9	33.9	0	0
0.25	5.40	22.6	0	0
Fineness modulus	2.79	2.38	5.68	6.72
Specific gravity	2.66	2.45	2.72	2.73

Table 3 Concrete mix proportions (kg/m³)

Mix ID	SF0R0	SF10R0	SF0R5	SF10R5	SF0R15	SF10R15	SF0R25	SF10R25
Cement	300	270	300	270	300	270	300	270
Silica fume* (%)	0	10	0	10	0	10	0	10
Silica fume	0	30	0	30	0	30	0	30
Water	180	180	180	180	180	180	180	180
SP**	4.5	4.8	4.9	5.5	5.8	6.3	6.8	7.2
Gravel	968	964	920	915	823	819	726	723
Sand	923	919	877	873	785	781	692	689
Rubber content*** (%)	0	0	5	5	15	15	25	25
Crumb rubber	0	0	14.8	14.7	44.3	44.1	73.8	73.5
Tire chips	0	0	18.2	18.1	54.5	54.2	90.8	90.4

* by total weight of binder; ** SP: Superplasticizer; *** by total volume of aggregate

were kept constant. Tire rubber was used as a replacement for an equal part of aggregate by volume. The rubberized concretes included both types of rubbers (crumb and tire chip) with three designated rubber contents of 5, 15, and 25% by total aggregate volume. The rubber content was divided equally between the crumb and tire chip. For example, for 50% rubber constituent, crumb rubber replaced 50% of the sand volume and tire chip replaced 50% of the coarse aggregate.

A total of 8 concrete batches was produced. Each batch was mixed according to ASTM C192 standard in a power-driven revolving pan mixer. The details of the concrete mixtures were given in Table 3. The control mixtures were designed to have slump values of 15±2 cm. The superplasticizer was used to achieve the specified slump at each concrete mixture. Three 150×150×150 mm cubic specimen, three Ø 150×300 cylindrical specimen and three Ø100×200 mm cylindrical specimen in which 16 mm diameter steel bar was centrally embedded were cast from each batch and compacted by a vibrating table. Test specimens were demoulded 24 h after casting and were tested after 28 days of water curing period.

2.3 Test methods

Water absorption by total immersion was measured according to ASTM C642-06 (2006). It is calculated by drying a sample to an unchanged mass, sinking it in water for a particular time and assessing its increase in mass as a percent of dry mass (Khatip and Clay 2004). In this study, the specimens were immersed in water for three days and then taken off from water to measure saturated surface dry weight (W_1). After the measuring of saturated surface dry weight, the specimens were placed in an oven till a constant mass was obtained. When the specimens reached the constant mass, the weight of the specimens were recorded (W_2). Water absorption for each sample was calculated by using Eq. 1. Test was conducted at the age of 28 days with three specimens for each concrete mixture, and the water absorption value, presented here, is the average of them.

$$WA(\%) = \left(\frac{W_1 - W_2}{W_2} \right) \times 100 \quad (1)$$

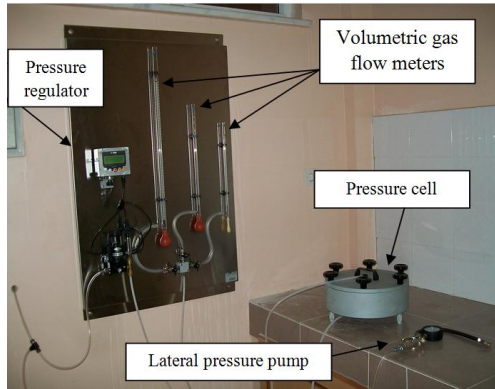
The CEMBUREAU method recommended by RILEM (1999) was used to investigate the gas permeability of the concretes. The photographic view and schematic representation as well as the detail of the testing cell are demonstrated in Fig. 1. A disk specimen having 50 mm height and 150 mm diameter, which were cut from the mid portion of $\emptyset 150 \times 300$ mm cylinder, were used to measure the gas permeability of the concretes. Oxygen gas was utilized as the permeating medium. The gas permeability coefficients were determined by applying the inlet gas pressures of 150, 200, and 300 kPa. Apparent gas permeability coefficient is average of these coefficients as recommended by RILEM (1999). After 28 days water curing period, the specimens used for the measuring of gas permeability coefficient were dried in oven and at each 6 hours the specimens were weighed till weight change was less than 1%. Then, they were kept in a sealed box till testing. Two disk specimens were tested at the age of 28 days and the average of them was reported as a test result.

For each differential pressure, Hagen-Poiseuille relationship for laminar flow of a compressible fluid through a porous media with small capillaries under steady-state condition was used to determine the apparent gas permeability coefficient K_g , which can be calculated using the modified Darcy's equation:

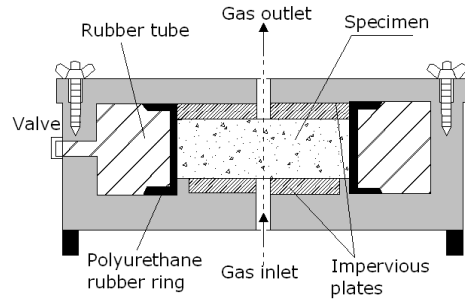
$$K_g = \frac{2P_2QL\mu}{A(P_1^2 - P_2^2)} \quad (2)$$

where K_g is the gas permeability coefficient (m^2), P_1 is the inlet gas pressure (N/m^2), P_2 is the outlet gas pressure (N/m^2), A is the cross-sectional area of the sample (m^2), L is the height of sample (m), μ is the viscosity of oxygen ($2.02 \times 10^{-5} Ns/m^2$), and Q is the volume flow rate (m^3/s).

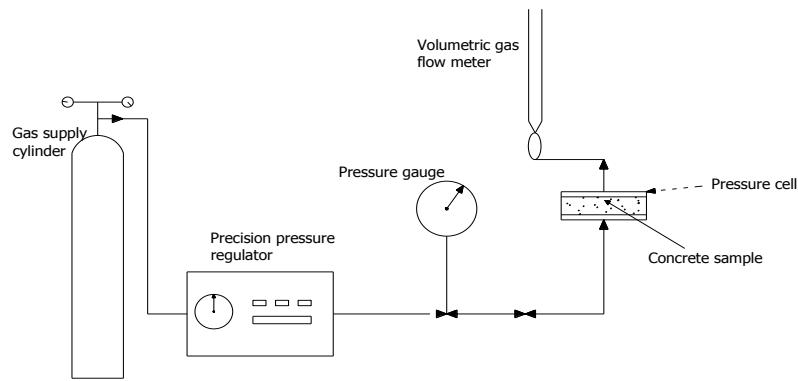
The water permeability of concretes was measured with respect to TS EN 12390-8 (2002). A 500 ± 50 kPa downward pressure was assigned on the specimens for 72 hours. After 72 hours, the specimens were split from the center point. Then, the largest penetration depth of water is measured in mm. When the concrete likely to come in contact with moderately aggressive media, the water does not penetrate to a depth of more than 50 mm. Whereas the water penetration depth



(a) photographic view of the gas permeability set up



(b) detail of pressure cell and test specimen



(c) schematic presentation of set-up

Fig. 1 Gas permeability test



(a) device



(b) measurement of penetration depth

Fig. 2 Water permeability test

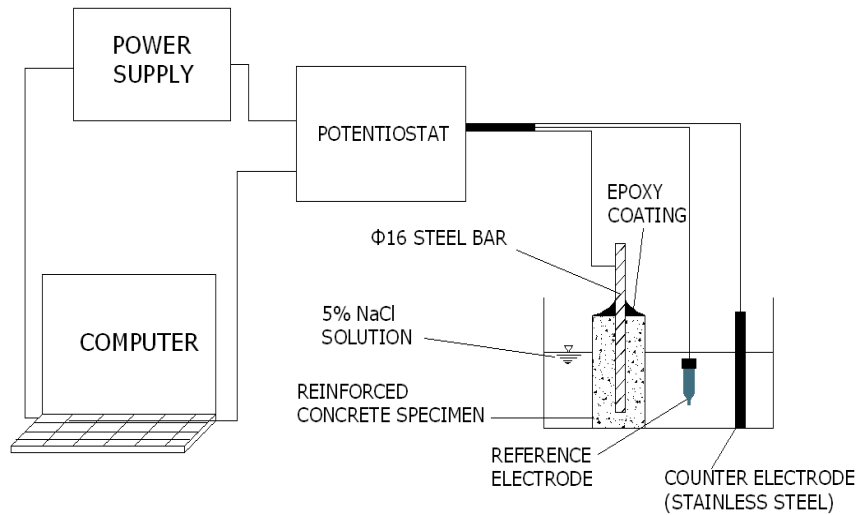


Fig. 3 Schematic presentation of the linear polarization resistance test set up

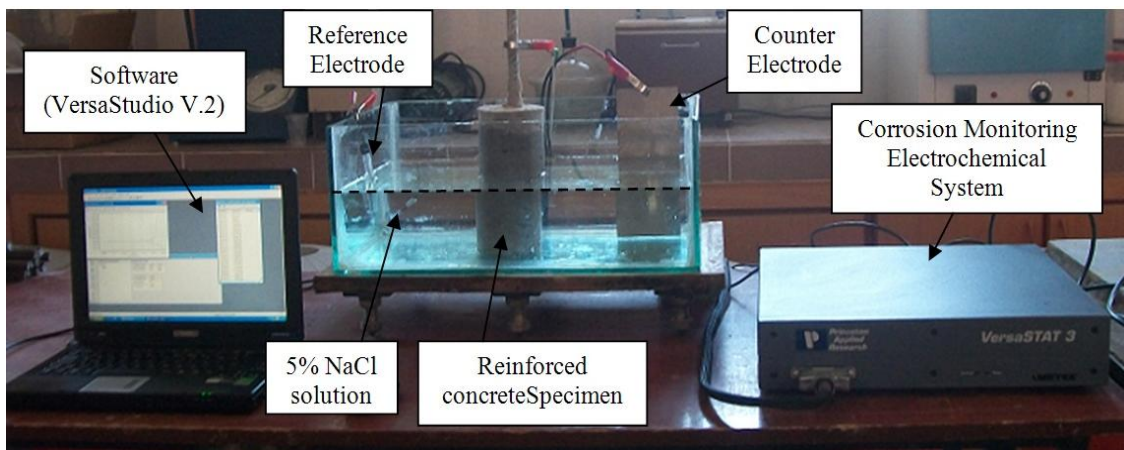


Fig. 4 Photographic view of the potentiostat/galvanostat test set up

is not more than 30 mm if concrete is likely to come in touch with aggressive media. A photographic view of the water permeability test equipment is given in Fig. 2.

VersaSTAT 3 a potentiostat/galvanostat with an optional frequency response analyzer (FRA) contained in a single unit was used to polarize the steel at a rate of 0.1 mV/s. Corrosion current density values of each mixture were calculated and presented. The test set up is schematically illustrated in Fig. 3. This test was applied to the concretes containing 10% silica fume and 5%, 15%, and 25% rubber aggregate as well as control samples. S420 reinforcement bar which is classified according to TS708 (2010) was used in this test. After 28 days of initial water curing, all concrete mixtures were immersed in 3% NaCl solution. Corrosion rate monitoring through linear polarization resistance method was carried out over 36 weeks of exposure. The photographic view

of the potentiostat/galvanostat test set up was also presented in Fig. 4.

Corrosion current density (I_{corr}) value of greater than $0.3 \mu\text{A}/\text{cm}^2$ indicates active corrosion, while a value less than $0.1 \mu\text{A}/\text{cm}^2$ means negligible corrosion (Rodriguez *et al.* 1994). Therefore, threshold criterion for corrosion initiation was selected as value of $0.3 \mu\text{A}/\text{cm}^2$. Direct current (DC) linear polarization resistance method with lower potentials was used to measure the corrosion current density. The resistance to polarization (R_p) was determined by conducting a linear polarization scan in the range of ± 25 mV of the open circuit potential at a scan rate of 0.1 mV per second. The Stern-Geary Formula (Eq. 3) was used to calculate the corrosion current density (I_{corr}) (Stern and Geary 1957) and 'B' in Eq. 3 calculated by the formula given in Eq. 4.

$$I_{corr}=B/R_p \quad (3)$$

$$B= (\beta_a\beta_c)/(2.303(\beta_a+\beta_c)) \quad (4)$$

where B is a constant based on the anodic and cathodic Tafel constants (β_a and β_c) and R_p is polarization resistance (Stern and Geary 1957). The value of B was taken as 26 mV considering steel in active condition (Maslehuddin and Al-Amoudi 1992).

According to Faraday's law, corrosion rate (CR) in mm/yr can be calculated by applying the following equation (Eq. 5) (Ismail and Ohtsu 2006).

$$\text{CR}=3.27\times I_{corr}\times\text{E.W.}/d \quad (5)$$

where EW is the equivalent weight of steel in gm and d is the density of reinforcing bar in g/cm^3 .

3. Test results and discussion

3.1 Water absorption

Water absorption of the concretes measured at the end of 28 days of water curing is demonstrated in Table 4. The variation in water absorption values range between 3.7% and 6.0% with respect to silica fume and rubber content. The water absorption values significantly decreased by the inclusion of silica fume as seen in Table 4. Increasing the rubber content, however, resulted in progressively increasing of the water absorption values. When the effect of increasing of rubber content investigated in the both concrete series, concrete with and without silica fume, almost same trend can be observed. Although the concrete with silica fume shown the better performance than concrete without silica fume for water absorption, as the rubber content increased, the difference between water absorption values of concrete with and without silica fume decreased and almost same values were observed at the 25% rubber content level. For the lower rubber content level, the effect of silica fume could be seen obviously. For example, water absorption value for plain concrete was measured as 4.1% while water absorption value for silica fume concrete is 3.7%. This indicates an significant improvement in absorption of concrete because of silica fume addition. A similar result was also observed in the study of Nili and Afroughsabet (2012). They reported that the concrete with a w/b ratio of 0.36 had about 1.8% water absorption, however, as a result of the use of 7.5% silica fume in concrete, water absorption was dropped to approximately 1.3%.

Table 4 Water absorption, water permeability and apparent gas permeability coefficients of plain and silica fume based rubberized concrete

Mixture ID	Water absorption, (%)	Water permeability, (mm)	Apparent gas permeability coefficient, $K \times 10^{-15}$, (m^2)
6SF0R0	4.11	47	1.35
6SF0R5	5.20	62	2.35
6SF0R15	5.56	111	NA*
6SF0R25	6.06	150	NA
6SF10R0	3.73	25	0.83
6SF10R5	4.15	40	2.06
6SF10R15	5.07	85	NA
6SF10R25	6.03	150	NA

*NA: not available

3.2 Gas permeability

Table 4 illustrates apparent gas permeability coefficients of rubberized concretes with and without silica fume. As it can be clearly seen from Table 4, the gas permeability test was conducted till 5% rubber replacement level. Due to high porosity of 15% and 25% replacements of rubber at both concrete series, the gas permeability test failed. Namely, due to very fast flow of oxygen through the specimen, the reading could not be taken from the volumetric gas flow meters. The gas permeability coefficients ranged from 0.83×10^{-15} to $2.35 \times 10^{-5} m^2$.

The maximum gas permeability coefficient was observed for SF0R5 while the minimum was measured at SF10R0. The utilization of SF enhanced the resistance of concrete against gas permeability as in water absorption. For example, the plain concrete without SF had gas permeability coefficient of $1.35 \times 10^{-15} m^2$, it was dropped to $0.83 \times 10^{-15} m^2$ as a result of SF incorporation. This may be attributed to the improved pore structure of the concrete as a result of contribution of SF by micro-filling and chemical effects (Al-Khaja 1994, Alexander and Magee 1999).

3.3 Water permeability

The variation in the water permeability of the plain and rubberized concretes is given in Table 4. The lowest water permeability value of 25 mm was achieved at SF10R0 concrete while the maximum 150 mm was observed at SF0R25 and SF10R25. Although the effect of SF could not be seen at 25% rubber content level, significant improvement in concretes containing lower rubber content as well as in the plain concrete was observed by addition of silica fume. For example, in the plain concrete without silica fume, water permeability value of 47 mm was obtained, when SF incorporated, this value dropped to 25 mm. The similar enhancement was achieved in rubber content of 5% and 15%. The plain concrete with silica fume is convenient to be used for the most of the structures under severe chemical effects. However, the plain concrete without silica fume and containing rubber had the water permeability values range from 40 mm to 150 mm. At this level of w/b ratio of 0.60, the utilization of rubber significantly increased the permeability depth and this makes concrete weak against chemical actions.

Due to the surface characteristic of rubber particles, the adhesion between rubber particles and matrix is low. This situation causes plenty of porosities. The porosities in concrete result in high

permeability characteristic (Gesoğlu and Güneyisi 2011). The higher porosity of concrete, the higher the water permeability. Moreover, in the literature many researchers recommend surface treatment of rubber particles to enhance their adhesion to the surrounding cement paste. Besides, utilization of tire chips, which has longitudinal shape and particle size of more than 4 mm, causes porosities in the concrete. Also, it has been suggested that utilization of ultrafine materials in the rubberized concrete production provides an increase in homogeneity and a decrease in the number of large pores in cement paste (Eldin and Serouci 1993a, Segre and Joekes 2000, Topçu 1995).

3.4 Corrosion resistance

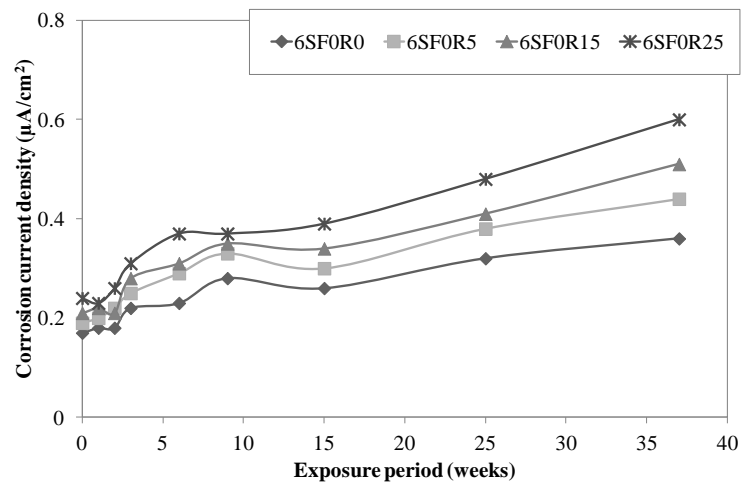
The variation in corrosion current densities (I_{corr}) of the rubberized concretes over 36 weeks of 3% NaCl exposure are shown in Fig. 5. Before the exposure, the corrosion current density was observed in the range of 0.14 to 0.24 $\mu\text{A}/\text{cm}^2$ for all concrete mixtures. During 36-week NaCl exposure period, increasing in the corrosion current density was observed in all concretes. However, the lowest I_{corr} values were pointed out in the concretes with silica fume based rubberized concrete. Utilization of rubber in the concrete caused increasing the corrosion current density values. Before chloride exposure, increasing the rubber content from 0% to 25% resulted in 41.2% and 42.9% increment in corrosion current density for plain and silica fume incorporated concrete series, respectively. Nevertheless, after 36-week chloride exposure period, increasing rubber content resulted in 66.7% and 70.6% increment in corrosion current density values for plain and silica fume incorporated concrete series, respectively.

As seen from Fig. 5, after nine-week chloride exposure, slight decrease in the corrosion current density values was observed in almost all mixtures and slight fluctuating was monitored at the beginning period of the chloride exposure. When the whole periods of corrosion current density were regarded, the continuous increasing could be seen clearly. Similar fluctuation in corrosion current density was also observed in the study of Kayalı and Zhu (2005). They carried out an experimental study on chloride diffusion and corrosion activity of reinforced silica fume-cement concrete slabs subjected to partial immersion in a 2% chloride solution. They observed continuous increase in I_{corr} values with slight fluctuations. Similarly, in the current study, the corrosion current density values began increasing after exposure and the highest values were observed at the end of 36-week chloride exposure. The highest values were obtained in 25% rubber content in concrete with and without silica fume as 0.58 and 0.60 $\mu\text{A}/\text{cm}^2$, respectively.

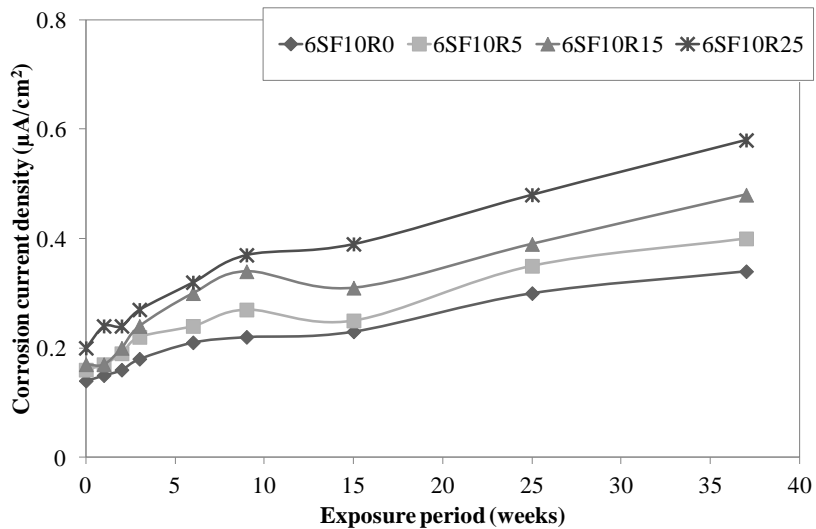
In the literature, the corrosion behavior of steel bar embedded in concrete according to the value of the corrosion current density result have been discussed discretely. The current density values which are greater than 0.3 $\mu\text{A}/\text{cm}^2$ have been stated as indicative of active corrosion by many researchers (Andrade *et al.* 1990, Al-Amoudi *et al.* 2003). However, in other study of Andrade and Alonso (2001), the corrosion behavior according to the value of corrosion current density stated as low for corrosion current density between 0.1 $\mu\text{A}/\text{cm}^2$ and 0.5 $\mu\text{A}/\text{cm}^2$ and as moderate for the values range between 0.5 and 1.0 $\mu\text{A}/\text{cm}^2$. The values greater than 1 $\mu\text{A}/\text{cm}^2$ and less than 0.1 $\mu\text{A}/\text{cm}^2$ were regarded as high and negligible, respectively (Andrade and Alonso 2001).

Based on the aforementioned information gathered from the technical literature, it can be concluded that there are several comments for corrosion resistance of concrete which is carried out according to LPR test. The corrosion resistance was defined discretely by each author. These remarks taken from literature were presented to get an idea about the corrosion behavior of the rubberized concretes dealt with this study. Besides, while the results obtained from this study can

be classified as moderate class for one author, they can be classified as high class for another author. For instance, while concretes including 5% and 15% rubber content and plain concrete mixtures fall into the low class at the end of 36-week chloride exposure period, concretes containing 25% rubber content falls into the low class till 25-week chloride exposure period and moderate class after 25-week chloride exposure period according to Andrade and Alonso (2001).



(a) rubberized concretes incorporating 0% SF



(b) rubberized concretes incorporating 10% SF

Fig. 5 Variation of corrosion current density over 36 weeks of 3% NaCl exposure

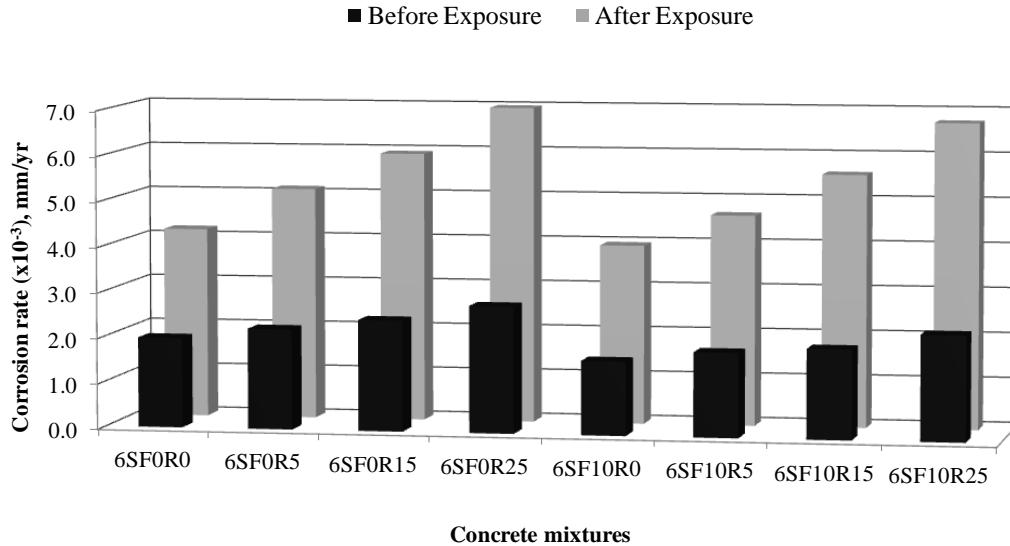


Fig. 6 The corrosion rate values before and after chloride exposure period of 36 weeks

The variation of the corrosion rate for different mixtures is showed in Fig. 6. As seen in Fig. 6, corrosion rate were significantly increased after 36-period of chloride exposure. The corrosion rates ranged between 0.0020 and 0.0028 mm/yr for plain rubberized concrete and 0.0016 and 0.0023 mm/yr for silica fume based rubberized concrete. After 36-week chloride exposure period, these values ranged between 0.0042 and 0.0070 mm/yr and 0.0039 and 0.0067 mm/yr for plain and silica fume based rubberized concrete series, respectively. Addition of the rubber to concrete and increasing its content caused significant increment in corrosion rate whereas incorporating the silica fume into rubberized concrete enhanced the corrosion rate. Silica fume utilization improved the corrosion rates of rubberized concrete as 18%, 16%, 19%, and 17% for rubber replacement level of 0%, 5%, 15%, and 25%, respectively.

4. Conclusions

Based on the findings presented in this study, the following conclusions can be drawn.

- The water absorption of rubberized concrete was observed to be decreased by utilization of silica fume. However, at 25% rubber content level, silica fume had a tendency to lose its effectiveness.
- The gas permeability coefficients of rubberized concrete were also reduced by silica fume addition. Moreover, after 5% rubber content, gas permeability test failed due to high amount of porosity.
- Water permeability of rubberized concrete reached the 150 mm, which is the dimension of test specimen, in both concrete with and without silica fume at 25% rubber content. However, silica fume had distinguishable effect on water permeability of concretes containing less than 25% rubber content.

- Corrosion current density values of the concretes seemed to have close trends with the aforementioned findings. The minimum corrosion current density values were measured in rubberized concretes incorporated with 10% silica fume. The values obtained for plain rubberized concretes were greater than silica fume based rubberized concretes before and after exposure.
- After nine-week NaCl exposure period, the corrosion current density values started to decrease with some fluctuations. Although decreasing in the corrosion current density was obtained with slight fluctuations, there was continuous rise in the corrosion current density when whole chloride exposure period was considered.
- The rate of corrosion was adversely affected by increasing the rubber content. Utilization of tyre in concrete production increases pores in concrete. These pores in the concrete are ways for penetration of water and oxygen to concrete. When the number of pores increases, the penetration of water and oxygen to concrete also increases. This situation adversely influences the corrosion resistance of the concrete. However, the use of silica fume enhanced the corrosion resistance of the rubberized concrete.

References

- Abu Bakar, B.H., Akil, H.M. and Ismail, H. (2013), "Experimental and numerical investigations of the influence of reducing cement by adding waste powder rubber on the impact behavior of concrete", *Comput. Concr.*, **11**(1), 63-73.
- Al-Amoudi, O.S.B., Maslehuddin, M., Lashari, A.N. and Almusallam A.A. (2003), "Effectiveness of corrosion inhibitors in contaminated concrete", *Cement Concrete Compos.*, **25**, 439-449.
- Alexander, M.G. and Magee, B.J. (1999), "Durability performance of concrete containing condensed silica fume", *Cement Concrete Res.*, **29**, 917-922.
- Ali, N.A., Amos, A.D. and Roberts, M. (1993) "Use of ground rubber tyres in portland cement concrete", *Proceeding of the International Conference: Concrete 2000—Economic and Durable Construction through Excellence*, University of Dundee, Scotland, UK, 1993.
- Al-Khaja, W.A. (1994), "Strength and time-dependent deformations of silica fume concrete for use in Bahrain", *Construct. Build. Mater.*, **8**, 169-172.
- Andrade, C. and Alonso, C. (2001), "On-site measurements of corrosion rate of reinforcements", *Constr. Build. Mater.*, **15**, 141-5.
- Andrade, C., Alonso, C. and Gonzalez, J.A. (1990), "An initial effort to use corrosion rate measurements for estimating rebar durability", In: Berke, N.S., Chaker, V. and Whiting, D. editors, *Corrosion rates of steel in concrete. ASTM STP 1065*, Philadelphia: American Society for Testing and Materials.
- ASTM C642-06 (2006), Standard test method for density, absorption, and voids in hardened concrete. Annual Book of ASTM Standards.
- Eldin, N.N. and Senouci, A.B. (1993a), "Rubber tire particles as concrete aggregate", *J. Mater. Civ. Eng. ASCE*, **5**(4), 478-496.
- Eldin, N.N. and Senouci, A.B. (1993b), "Observations on rubberized concrete behavior", *Cement Concr. Aggr.*, **15**(1), 74-84.
- Eldin, N.N. and Senouci, A.B. (1994), "Measurement and prediction of the strength of rubberized concrete", *Cement Concrete Compos.*, **16**, 287-298.
- Feldman, R.F. and Huang, C.Y. (1985), "Properties of portland cement silica fume paste: II. Mechanical properties", *Cement Concrete Res.*, **15**(6), 943-952.
- Gesoğlu, M. and Güneyisi, E. (2007), "Strength development and chloride penetration in rubberized concretes with and without silica fume", *Mater. Struct.*, **40**, 953-964
- Gesoğlu, M. and Güneyisi, E. (2011), "Permeability properties of self-compacting rubberized concretes",

- Construct. Build. Mater.*, **25**, 3319-3326.
- Güneysi, E., Gesoğlu, M. and Özturan, T. (2004), "Properties of rubberized concretes containing silica fume", *Cement Concrete Res.*, **34**, 2309-2317.
- Inthata, S. and Cheerarat, R. (2014), "Chloride penetration resistance of concrete containing ground fly ash, bottom ash and rice husk ash", *Comput. Concr.*, DOI: 10.12989/cac.2014.13.1.017.
- Ismail, M. and Ohtsu, M. (2006), "Corrosion rates of steel in concrete", *Cement Concrete Res.*, **16**, 771-781.
- Issa, C.A. and Salem, G. (2013), "Utilization of recycled crumb rubber as fine aggregates in concrete mix design", *Construct. Build. Mater.*, **42**, 48-52.
- Kayali, O.A. and Zhu, B. (2005), "Corrosion performance of medium-strength and silica fume high-strength reinforced concrete in a chloride solution", *Cement Concrete Compos.*, **27**, 117-124.
- Khatip, J.M. and Clay, R.M. (2004), "Absorption characteristics of metakaolin concrete", *Cement Concrete Res.*, **34**, 19-29.
- Khatip, Z.K. and Bayomy, F.M. (1999), "Rubberized Portland cement concrete", *J Mater Civil Eng ASCE*, **11**(3), 206-213.
- Lee, B.I., Burnett, L., Miller, T., Postage, B. and Cuneo, J. (1993), "Tyre rubber cement matrix composites", *J. Mater. Sci. Lett.*, **12**(13), 967-968.
- Li, Z., Li, F. and Li, J.S.L. (1998), "Properties of concrete incorporating rubber tyre particles", *Mag. Concr. Res.*, **50**(4), 297-304.
- Maslehuddin, M. and Al-Amoudi O.S.B. (1992), "Corrosion of reinforcing steel in concrete: its monitoring and prevention", *Preprint, Symposium on Corrosion and its Control*, King Saud University, Riyadh.
- Mehta, P.K. and Gjørv, O.E. (1982), "Properties of portland cement concrete containing fly ash and condensed silica fume", *Cement Concrete Res.*, **12**(5), 587-595.
- Mindess S (1994), *Material Selection, Proportioning, and Quality Control, High Performance Concretes and Applications*, Edward Arnold, London, England.
- Nili, M. and Afroughsabet, V. (2012), "Property assessment of steel-fibre reinforced concrete made with silica fume", *Construct. Build. Mater.*, **28**, 664-669.
- Parande, A.K. (2013), "Role of ingredients for high strength and high performance concrete – a review", *Adv. Concrete Construct.*, **1**(2), 151-162.
- Raghavan, D., Huynh, H. and Ferraris, C.F. (1998), "Workability, mechanical properties, and chemical stability of a recycled tyre rubber filled cementitious composite", *J. Mater. Sci.*, **33**, 1745-1752.
- Rahman, M.M., Usman, M. and Al-Ghalib, A.A. (2012), "Fundamental properties of rubber modified self-compacting concrete", *Construct. Build. Mater.*, **36**, 630-637.
- Rebeiz, K.S., Fowler, D.W. and Paul, D.R. (1992), "Polymer concrete and polymer mortar using resins based on recycled polyethylene terephthalate", *J Appl. Polym. Sci.*, **44**(9), 1649-1655.
- Rebeiz, K.S., Serhal, S. and Fowler, D.W. (1993), "Shear behavior of steel reinforced polymer concrete using recycled plastic", *ACI Struct. J.*, **90**(6), 675-682.
- Rebeiz, K.S., Yang, S. and Fowler, D.W. (1994), "Polymer mortar composites made with recycled plastics", *ACI Mater. J.*, **91**(3), 313-319.
- RILEM TC 116-PCD (1999), Permeability of concrete as a criterion of its durability, *Mater. Struct.*, **32**, 174-179.
- Rodriguez, P., Ramirez, E. and Honzalez, J.A. (1994), "Methods for studying corrosion in reinforced concrete", *Mag. Concr. Res.*, **46**, 81-90.
- Rostami, H., Lepore, J., Silverstrim, T. and Zandi, I. (1993) "Use of recycled rubber tyres in concrete", *Proceeding of the International Conference: Concrete 2000—Economic and Durable Construction through Excellence*, University of Dundee, Scotland, UK.
- Savaş, B.Z., Ahmad, S. and Fedroff, D. (1996), "Freeze-thaw durability of concrete with ground waste tire rubber", *Transportation Research Board*, Washington, DC.
- Segre, N. and Joekes, I. (2000), "Use of tire rubber particles and addition to cement paste", *Cement Concrete Res.*, **30**, 1421-1425.
- Siddique, R. and Naik, T.R. (2004), "Properties of concrete containing scrap-tire rubber-an overview", *Waste Manag.*, **24**, 563-569.

- Soroushian, P., Plasencia, J. and Ravanbakhsh, S. (2003), "Assessment of reinforcing effects of recycled plastic and paper in concrete", *ACI Mater. J.*, **100**(3), 203-207.
- Stern, M. and Geary, A.L. (1957), "A theoretical analysis of the slope of the polarization curves", *J Electrochem. Soc.*, **104**, 56-63.
- Sukontasukkul, P. and Chaikaew, C. (2006), "Properties of concrete pedestrian block mixed with crumb rubber", *Construct. Build. Mater.*, **20**, 450-457.
- Topçu, I.B. (1995), "The properties of rubberized concretes", *Cement Concrete Res.*, **25**(2), 304-310.
- Topçu, I.B. (1997), "Assesment of the brittleness index of rubberized concrete", *Cement Concrete Res.*, **27**(2), 177-183.
- Topçu, I.B. and Avcular, N. (1997), "Collosion behaviours of rubberized concrete", *Cement Concrete Res.*, **27**(12), 1893-1898.
- Toutanji, H.A. (1996), "The use rubber tire particles in concrete to replace mineral aggregates", *Cement Concrete Compos.*, **18**, 135-139.
- TS708 (2010), Çelik - betonarme için - donatı çeliği, Institute of Turkish Standards, Ankara, Turkey.
- TS-EN 12390-8 (2002), Testing Hardened Concrete-Part 8: Depth of Penetration of Water under Pressure. Institute of Turkish Standards, Ankara, Turkey.
- Wang, C., Zhang, Y. and Zhao Z. (2012), "Fracture process of rubberized concrete by fictitious crack model and AE monitoring", *Comput. Concr.*, **9**(1), 51-61.
- Wang, Y., Zureick, A.H. and Cho, B.S. (1994), "Properties of fibre reinforced concrete using recycled fibres from carpet industrial waste", *J. Mater. Sci.*, **29**(16), 4191-4199.
- Wu, H.C., Lim, Y.M. and Li, V.C. (1996), "Application of recycled tyre cord in concrete for shrinkage crack control", *J. Mater. Sci. Lett.*, **15**, 1828-1831.
- Yung, W.H., Yung, L.C. and Hua, L.H. (2013), "A study of the durability properties of waste tire rubber applied to self-compacting concrete", *Construct. Build. Mater.*, **41**, 665-672.